Electronic Supplementary Material (ESI) for Journal of Materials Chemistry A.


# Supporting Information

## Organic polymeric filler-amorphized poly(ethylene oxide) electrolyte enables all-solid-state lithium-metal batteries operating at 35 °C

*Gulian Wang,[a†] Xingyu Zhu,[a†] Arif Rashid,[a] Zhongli Hu,[a] Pengfei Sun,[a] Qiaobao Zhang*[b] and Li Zhang*[a]*

[a.] *College of Energy, Soochow Institute for Energy and Materials InnovationS, Soochow University, Suzhou 215006, China. E-mail: zhangli81@suda.edu.cn*

[b.] *Department of Materials Science and Engineering, College of Materials, Xiamen University, Xiamen 361005, Fujian, China. E-mail: zhangqiaobao@xmu.edu.cn*

[†]*These authors contributed equally to this work.*

## Supplementary Figures

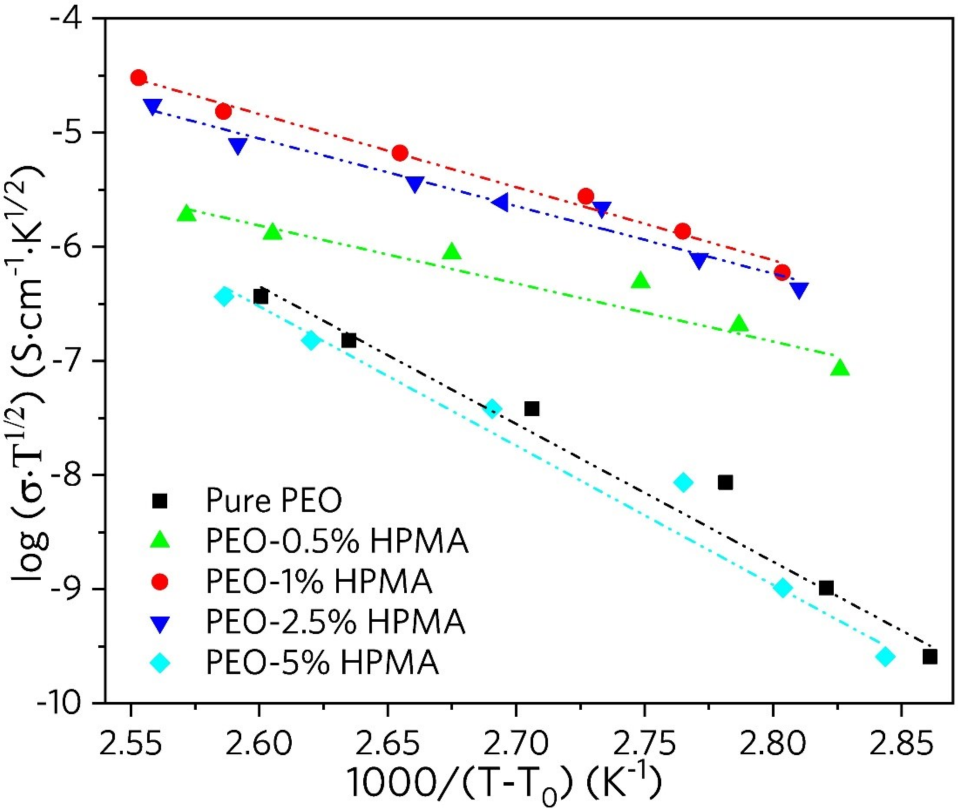


**Figure S1**. Plots of log ($\sigma \cdot T^{1/2}$) *vs*. 1000/($T$-$T_0$) of the pristine PEO and PEO-HPMA SPEs with different HPMA dosages.

As displayed in Figure 3a, the plots of log $\sigma$ versus $T^{-1}$ for the pristine PEO and PEO-HPMA SPEs with different HPMA dosages present a non-liner relationship, which can be further described by the Vogel-Tamman-Fulcher (VTF) empirical equation (Ref: *Angew. Chem. Int. Ed.*, 2018, **57**, 10168-10172)

$$\sigma = \sigma_0 T^{-1/2} \exp(-\frac{E_a}{T - T_0})$$

Where $\sigma_0$ is the pre-exponential factor, $E_a$ is the activation energy, $T_0$ is a parameter correlated to the glass transition temperature $T_g$, and R is the ideal gas constant. Herein, we use the $T_g$ values obtained from the DSC tests (Figure 2e) to approximate the $T_0$. By linearly fitting the log ($\sigma \cdot T^{1/2}$) *vs.* 1000/($T$-$T_0$) relationship, the $E_a$ of the PEO-1%HPMA SPE is calculated to be 0.53 eV, while the pristine PEO shows a much higher value of 1.01 eV. Generally, a lower $E_a$ represents $Li^+$ ions that requires less energy when moving in the electrolyte, *i.e.*, a higher ionic conductivity.




Please do not adjust margins

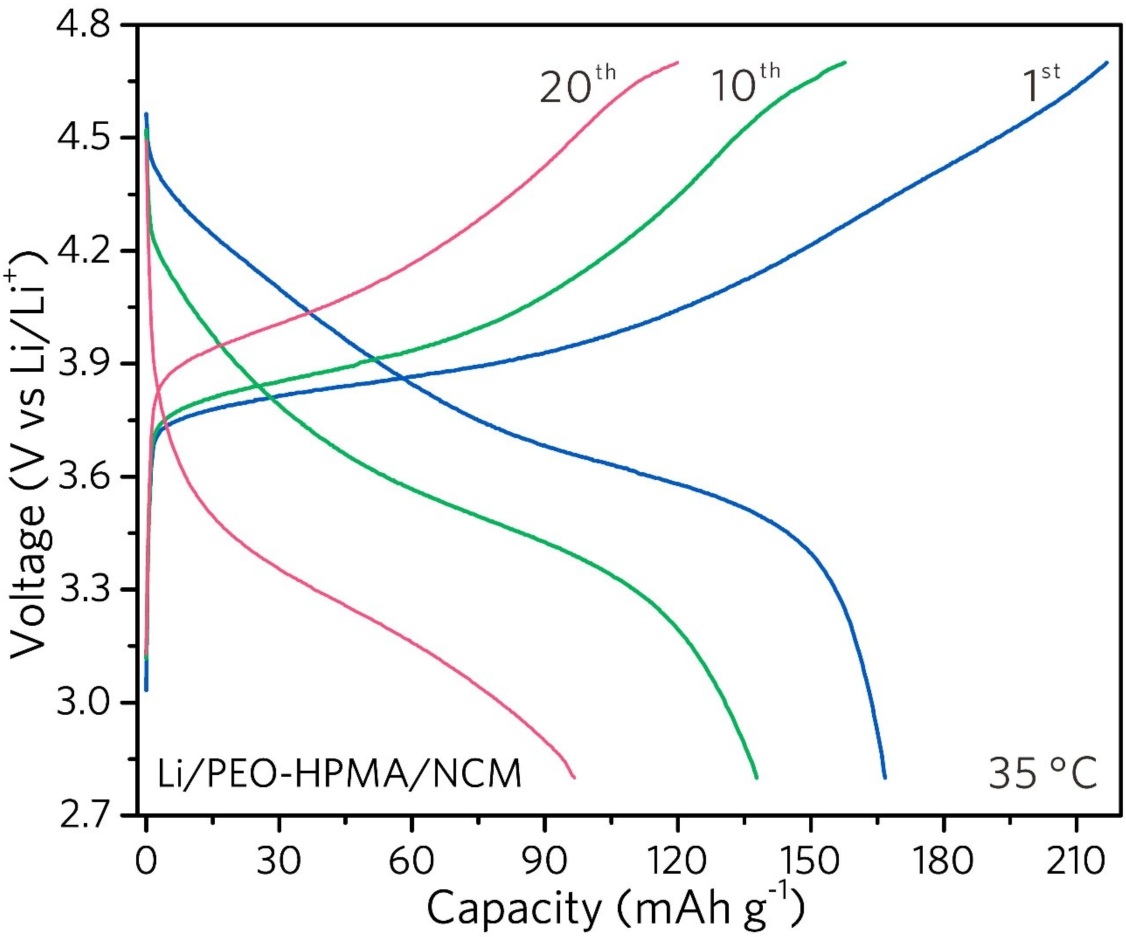


**Figure S2**. Charge/discharge profiles of the Li/PEO-1% HPMA/$LiNi_{0.5}Co_{0.2}Mn_{0.3}O_2$ cell after various cycles at 0.1 C.

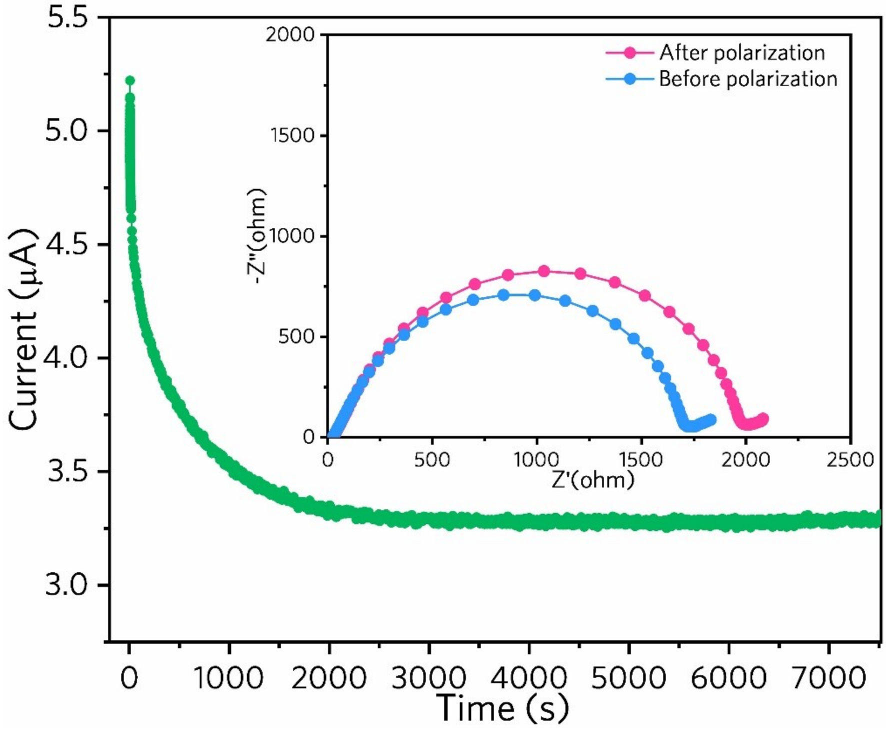


**Figure S3**. The chronoamperometry profile of a symmetrical Li/PEO-1% HPMA/Li cell under a polarization voltage of 10 mV. The inset shows the Nyquist profiles of the cell before and after the chronoamperometry test.

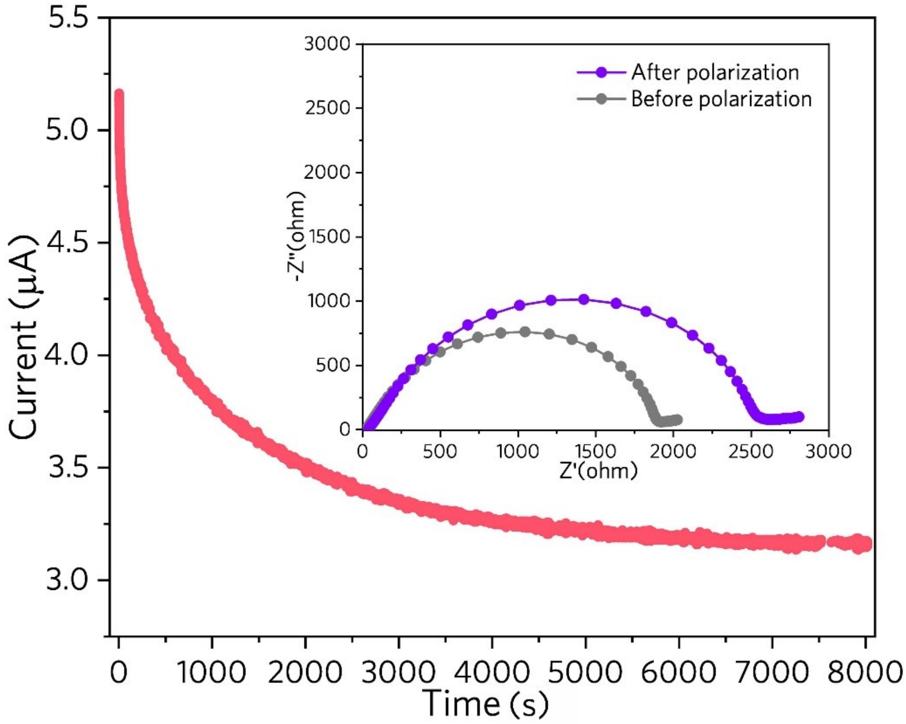


**Figure S4**. The chronoamperometry profile of a symmetrical Li/PEO /Li cell under a polarization voltage of 10 mV. The inset shows the Nyquist profiles of the cell before and after the chronoamperometry test.




Please do not adjust margins

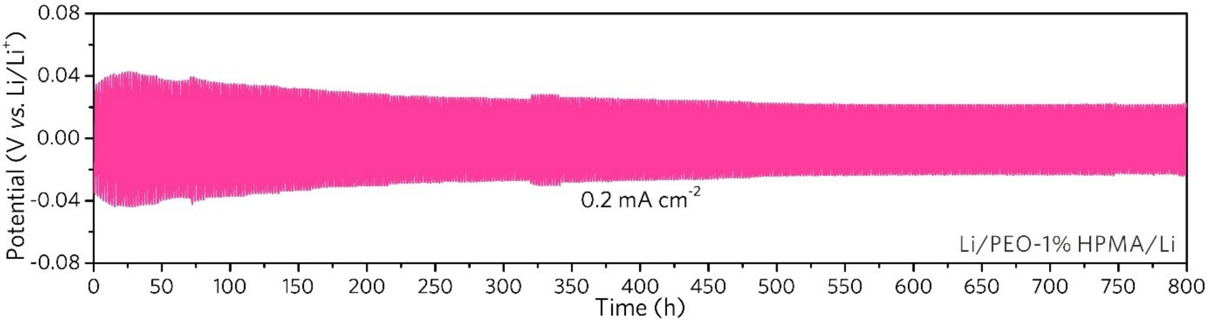


**Figure S5**. Voltage versus time profile of the symmetrical Li/PEO-1% HPMA/Li cell during the repeated Li plating/stripping process at current densities of 0.2 mA $cm^{-2}$.

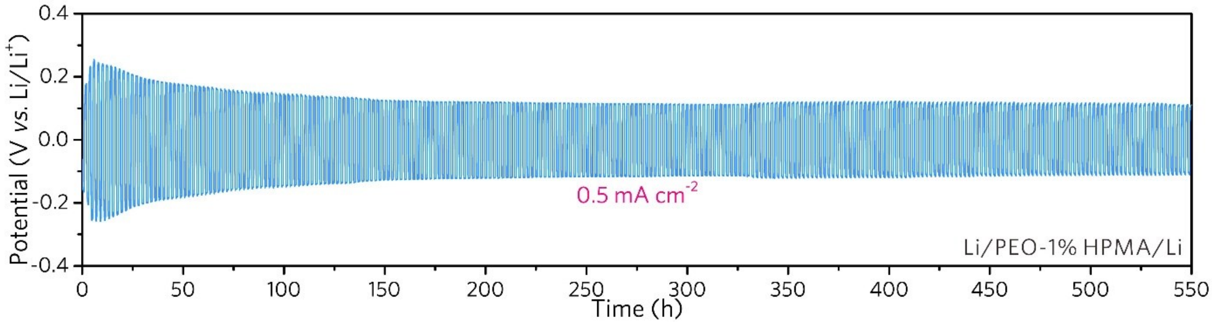


**Figure S6**. Voltage versus time profile of the symmetrical Li/PEO-1% HPMA/Li cell during the repeated Li plating/stripping process at current densities of 0.5 mA $cm^{-2}$.

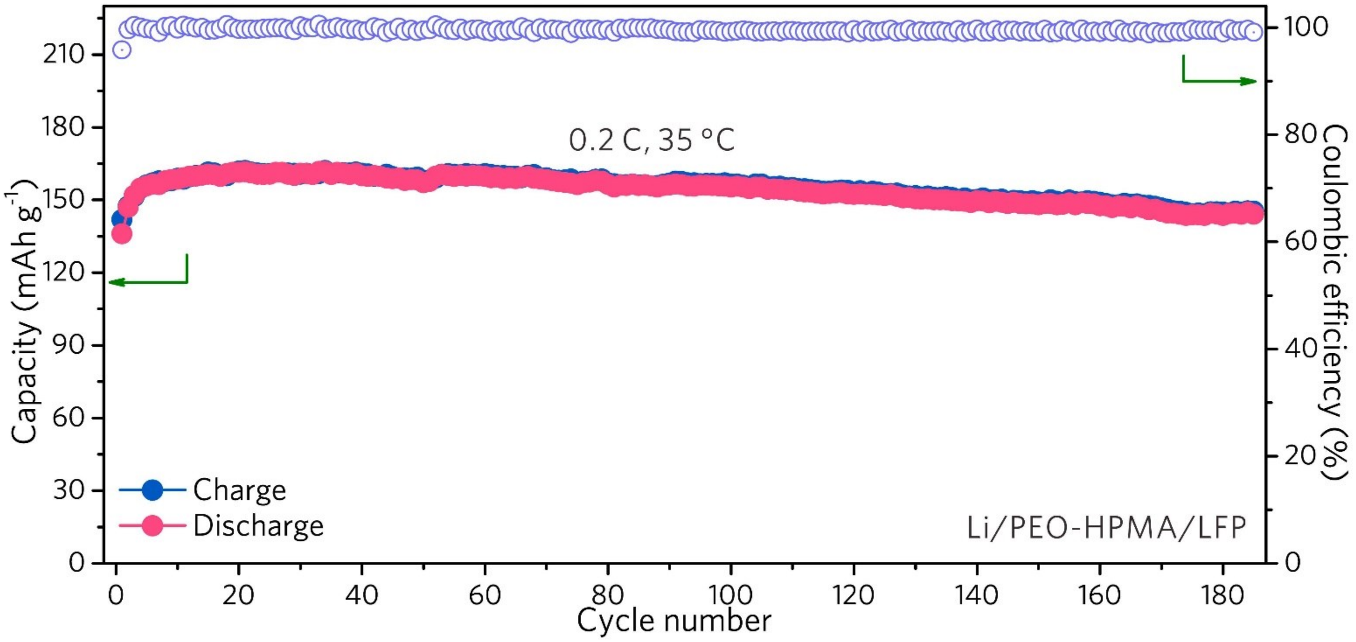


**Figure S7**. Long-term cycling stability of the Li/PEO-HPMA/LFP cell in a potential range of 2.6-4.3 V at a current rate of 0.2 C and corresponding Coulombic efficiency vs. cycle number profile.

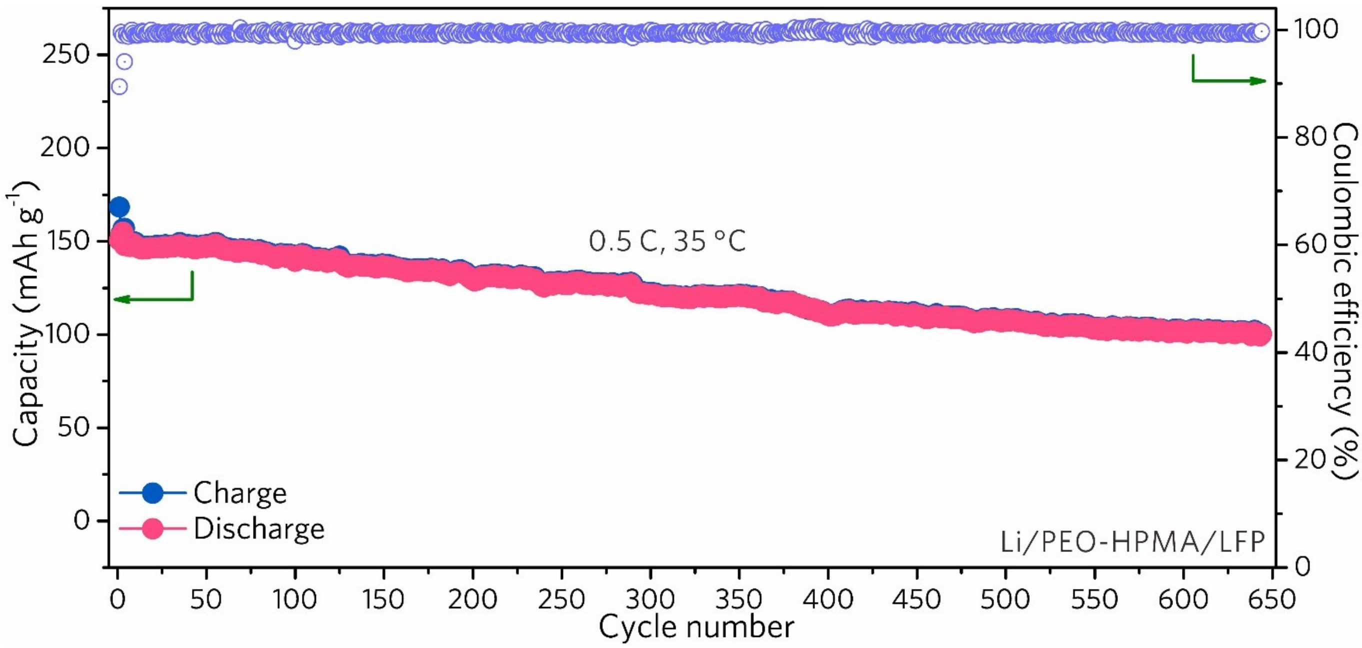


**Figure S8**. Long-term cycling stability of the Li/PEO-HPMA/LFP cell in a potential range of 2.6-4.3 V at a current rate of 0.5 C and corresponding Coulombic efficiency vs. cycle number profile.

 

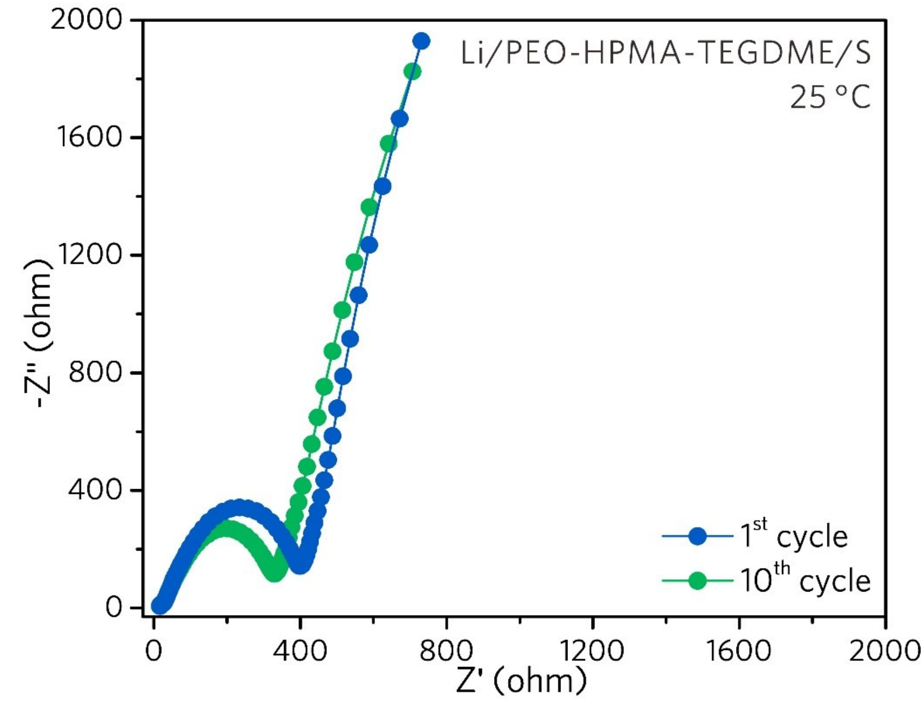


**Figure S9**. Nyquist plot of the quasi-solid-state Li-S battery after cycling for 1 and 10 cycles, respectively.

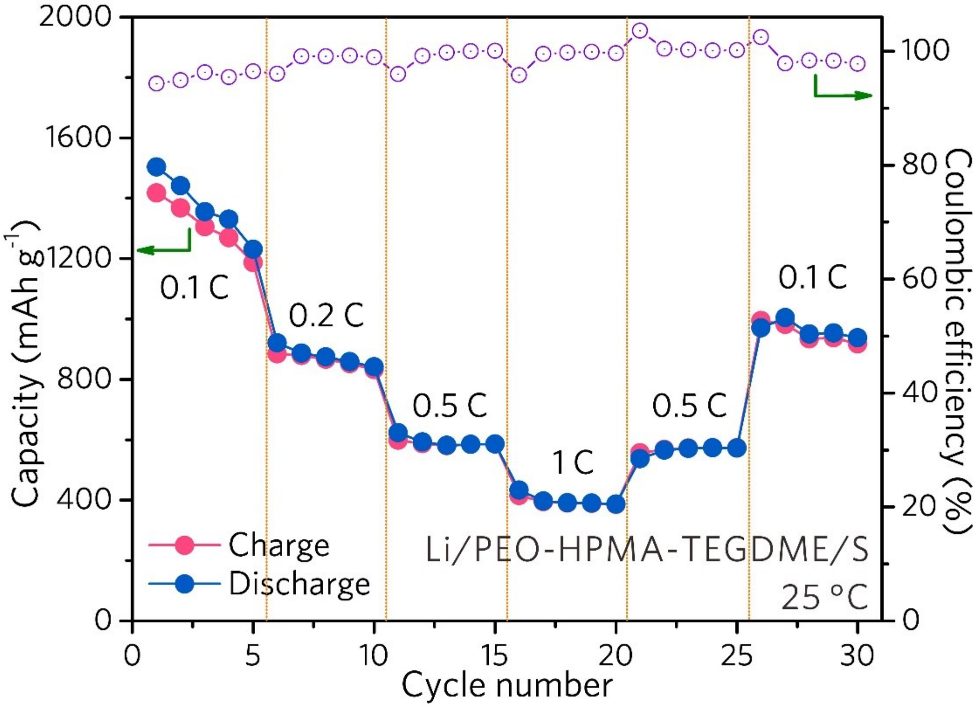


**Figure S10**. Rate capability of Li/PEO-HPMA-TEGDME/S cells at various current rates from 0.1 to 1 C (1C= 1675 mA $g^{-1}$).

**Table S1**. Comparison of the ionic conductivity, electrochemical performance and operating temperature between our PEO-HPMA SPE and the state-of-the-art PEO-based SPEs in the literatures.

| PEO-based SPEs | Ionic conductivity (S $cm^{-1}$) | Active materials | Electrochemical performance and operating temperature | Refs |
|---|---|---|---|---|
| **PEO/LiTFSI+ HPMA** | 1.13*$10^{-4}$ at 35 °C<br>2.16*$10^{-4}$ at 45 °C | $LiFePO_4$ | 160.3, 150.5 and 143.8 mAh·$g^{-1}$ at 0.1, 0.5 and 1 C, **35 °C**<br>144.1 mAh·$g^{-1}$ after 185 cycles at 0.2 C, **35 °C** | This work |
| PEO/LiTFSI+ $BaTiO_3$ nanospheres | 1.8*$10^{-5}$ at 25 °C<br>1.6*$10^{-3}$ at 80 °C | $LiFePO_4$ | 135.6 mAh·$g^{-1}$ at 0.1C, **80 °C**<br>97.5% capacity retention after 50 cycles | [1] |
| $LiClO_4$/PEO+ LLTO nanofiber | 4.01*$10^{-4}$ at 60 °C | $LiFePO_4$ | 140 mAh·$g^{-1}$ at 1C, **60 °C**<br>92.4% capacity retention after 100 cycles | [2] |
| PEO/LiTFSI+ LLZO NWs | 2.39*$10^{-4}$ at 25 °C<br>1.15*$10^{-3}$ at 60 °C | $LiFePO_4$ | 158.7 mAh·$g^{-1}$ after 80 cycles at 0.1 C, **45 °C**<br>158.8 mAh·$g^{-1}$ after 70 cycles at 0.5 C, **60 °C** | [3] |
| PEO/LiTFSI + nanoporous SSZ-13 | 1.91*$10^{-3}$ at 60 °C<br>4.43*$10^{-5}$ at 20 °C | $LiFePO_4$ | 130 mAh·$g^{-1}$ after 100 cycles at 1C, **58 °C** | [4] |
| PEO/LiTFSI + g-$C_3N_4$ | 1.7*$10^{-5}$ at 30 °C | $LiFePO_4$ | 155 mAh·$g^{-1}$ after 100 cycles at 0.2 C, **60 °C** | [5] |
| PEO/LiTFSI + LAGP | -- | $LiFePO_4$ | ~120 mAh·$g^{-1}$ at 1C and 70% retention after 500 cycles, **30 °C** | [6] |
| PEO/LiTFSI +7.5%LLZO | 5.5*$10^{-4}$ at 30 °C | $LiFePO_4$ | ~150 mAh·$g^{-1}$ at 0.1 C, **60 °C** | [7] |
| PEO/LiTFSI+ LSTZ | 3.5*$10^{-4}$ at 45 °C | $LiNi_{0.8}Mn_{0.1}Co_{0.1}O_2$ | 151, 125 and 100 mAh·$g^{-1}$ delivered at 50,100 and 150 uA·$cm^{-2}$, **45 °C** | [8] |
| PEO/LiTFSI+ LSTZ | 3.5*$10^{-4}$ at 45 °C | $LiFePO_4$ | 156, 149 and 128 mAh·$g^{-1}$ delivered at 50,100 and 200 uA·$cm^{-2}$, **45 °C** | [8] |

**References in Table S1.**

(1) Y. Zhang, X. Wang, W. Feng, Y. Zhen, P. Zhao, Z. Cai and L. Li, *Ionics,* **2018**, *25*, 1471.

 

(2) K.-Q. He, J.-W. Zha, P. Du, S.-H. Cheng, C. Liu, Z.-M. Dang and R. K. Li, *Dalton Trans.*, DOI: 10.1039/C9DT00074G.

(3) Z. Wan, D. Lei, W. Yang, C. Liu, K. Shi, X. Hao, L. Shen, W. Lv, B. Li, Q.-H. Yang, F. Kang and Y.-B. He, *Adv. Funct. Mater.,* **2019**, *29*, 1805301.

(4) W. Li, S. Zhang, B. Wang, S. Gu, D. Xu, J. Wang, C. Chen and Z. Wen, *ACS Appl. Mater.Interfaces,* **2018**, *10*, 23874.

(5) Z. Sun, Y. Li, S. Zhang, L. Shi, H. Wu, H. Bu and S. Ding, *J. Mater. Chem. A*, DOI: 10.1039/C9TA00634F.

(6) C. Fu, S. Lou, Y. Cao, Y. Ma, C. Du, P. Zuo, X. Cheng, W. Tang, Y. Wu, Y. Gao, H. Huo and G. Yin, *Electrochim. Acta,* **2018**, *283*, 1261.

(7) F. Chen, D. Yang, W. Zha, B. Zhu, Y. Zhang, J. Li, Y. Gu, Q. Shen, L. Zhang and D. R. Sadoway, *Electrochim. Acta,* **2017**, *258*, 1106.

(8) H. Xu, P.-H. Chien, J. Shi, Y. Li, N. Wu, Y. Liu, Y.-Y. Hu and J. B.Goodenough, *PNAS,* **2019**, *116*, 18815.





Please do not adjust margins